

RADIATION FROM LARGE POOL FIRES

Shokri, M., and Beyler, C.L.*
Center for Firesafety Studies
Worcester Polytechnic Institute
Worcester, MA 01609

SUMMARY

Through a review of available data for radiation from large pool fires to external targets, a procedure for predicting the incident radiant flux to a target outside the flame is developed. The procedure is based on the classic cylindrical flame shape assumption and uses the flame height expression developed by Heskestad. The 'effective' emissive power of the flame is found through direct comparison of model predictions with experimental data. The 'effective' emissive power is found to decrease with increasing pool diameter. The results are compared to the method of Mudan and Croce described in the *SFPE Handbook of Fire Protection Engineering*, and the present method is shown to provide more accurate predictions of radiant heat flux from large pool fires. A complete procedure for determining radiative heating of a target subjected to radiation from a pool fire is presented.

The Orloff and deRis model for radiative heat transfer from the flame to the pool surface is clarified and simplified.

INTRODUCTION

Radiation from pool fires is well known to dominate other modes of heat transfer for pool diameters of 0.3-0.5 m or more. There have been many experimental studies of large pool fire structure and radiation¹⁻¹⁴. It is the purpose of this investigation to develop simple methods for the prediction of radiation from pool fires based on pool fire radiation data available in the open literature. Only data for pool fires in excess of one meter diameter will be considered.

In this investigation experimental data for pool fire radiation to external targets will be used to test the classical cylindrical flame radiation model and determine the 'effective' emissive power required in this model to achieve the best fit with available data. A full algorithm for prediction including required constants is developed and the method is compared with the method of Mudan and Croce²³.

A model for radiative transfer from the flame to the pool surface will also be developed from the model of Orloff and deRis²⁵.

METHOD

The correlation of flame radiation to external

*Current address for correspondence: Dr. Craig Beyler, Fire Science Technologies, 5430F Lynx Lane, Suite 131, Columbia, MD 21044

targets requires a simple yet realistic model of the flame. Towards this end the flame is assumed to be a cylindrical, blackbody homogeneous radiator. The incident radiative flux to a target outside the flame, \dot{q}'' , is given by

$$\dot{q}'' = EF_{12} \quad (1)$$

where E is the 'effective' emissive power of the flame and F_{12} is the configuration factor between the target and the flame. No explicit correction for atmospheric absorption of radiation will be made.

The configuration factor is solely a function of the target location and the flame height and diameter. The diameter of the cylinder is the pool diameter, D , and the flame height, H , is determined from the flame height correlation of Heskestad¹⁵. For noncircular pools the 'effective' diameter will be defined as the diameter of a circular pool with an area equal to the actual pool area, i.e.

$$D = \sqrt{\frac{4A}{\pi}} \quad (2)$$

Other models will be required for pools with aspect ratios greater than 2.5⁹.

Correlations, which describe the effect of pool diameter and burning rate on flame height, have been reviewed in Reference 16. Of the available correlations, the Heskestad expression

best fits the available large diameter, low H/D pool fires. At the same time, this correlation also reproduces the well known large H/D asymptotic behavior, where the flame height is dependent only on the heat release rate. Given the excellent performance of the Heskestad correlation over a wide range of conditions, it is selected for use here in the form

$$H = 0.23 \dot{Q}^{2/5} - 1.02 D \quad (3)$$

where \dot{Q} is in kW and D is in meters. This equation requires that the heat release rate be known.

Babrauskas¹⁷ has reviewed pool burning rate data and correlations. He recommends that the heat release rate, \dot{Q} , can be determined as follows

$$\dot{m}'' = \dot{m}_{\infty}'' [1 - \exp(-k\beta D)]$$

$$\dot{Q} = \Delta h_c \dot{m}'' A \quad (4)$$

where \dot{m}_{∞}'' and $k\beta$ are properties of the fuel, \dot{m}'' is the mass volatilization rate per unit area, A is the pool surface area, and Δh_c is the lower heat of combustion. This model is used here with fuel parameters, \dot{m}_{∞}'' and $k\beta$, taken from References 17,18 as determined by Babrauskas. For fuels for which these parameters have not been tabulated, \dot{m}_{∞}'' may be estimated by the Mudan expression¹⁸

$$\dot{m}_{\infty}'' = 10^{-3} \left(\frac{\Delta h_c}{\Delta h_v} \right) \quad (5)$$

where Δh_v is the heat required to heat the liquid fuel to the boiling temperature plus the heat of vaporization at the boiling temperature. For pool diameters of several meters or more, it is generally suitable to take $\dot{m}'' = \dot{m}_{\infty}''$.

Given the diameter and height of the flame, the configuration factor can be determined using widely published results for F_{12} from vertical cylindrical radiation sources¹⁹⁻²⁰. The formulas for horizontal and vertical targets are reproduced below.

$$F_{12,H} = \frac{(B-1/S)}{\pi\sqrt{B^2-1}} \tan^{-1} \sqrt{\frac{(B+1)(S-1)}{(B-1)(S+1)}} - \frac{(A-1/S)}{\pi\sqrt{A^2-1}} \tan^{-1} \sqrt{\frac{(A+1)(S-1)}{(A-1)(S+1)}} \quad (6a)$$

$$F_{12,v} = \frac{1}{\pi S} \tan^{-1} \left(\frac{h}{\sqrt{S^2-1}} \right) - \frac{h}{\pi S} \tan^{-1} \sqrt{\frac{(S-1)}{(S+1)}} + \frac{A h}{\pi S \sqrt{A^2-1}} \tan^{-1} \sqrt{\frac{(A+1)(S-1)}{(A-1)(S+1)}} \quad (6b)$$

where,

$$S = \frac{2L}{D}, \quad h = \frac{2H}{D}$$

$$A = \frac{(h^2 + S^2 + 1)}{2S}$$

$$B = \frac{1 + S^2}{2S}$$

The maximum configuration factor at a point is given by the vectoral sum of the horizontal and vertical configuration factors.

$$F_{12,max} = \sqrt{F_{12,H}^2 + F_{12,v}^2} \quad (7)$$

In this investigation all experimental results are for vertical targets, so Equation 6b is used.

The 'effective' emissive power of the flame will be determined by comparison with a wide range of experimental measurements of radiant flux from pool fires to external targets¹⁻⁶. It is important to note that the 'effective' emissive power of the flame is defined only in terms of a homogeneous flame radiation model. It is not the local emissive power which can be measured directly with a narrow angle radiometer. The determination of the 'effective' emissive power can only be made by the comparison of radiant heat flux data with a fully specified radiation model. It includes effects of smoke obscuration of the flame as well as any deficiencies elsewhere in the radiation model. Since emissive power is generally measured in the center of the flame with a narrow angle radiometer, the 'effective' emissive power is generally less than local measured emissive powers. These local and 'effective' emissive powers are very different and cannot be used interchangeably.

To summarize the model proposed here, the heat release rate is estimated from Equation 4 which is used in Equation 3 to find the flame height. The flame diameter is taken equal to the pool diameter or the 'effective' pool diameter of noncircular pools as given by Equation 2. Using the flame diameter and height, Equation 6b gives the configuration factor. No corrections for atmo-

spheric absorption of radiation are made. The 'effective' emissive power of the flame will be determined using Equation 1 by fitting experimental measurements of radiant flux from pool fires to external targets from References¹⁻⁶.

DATA

The data utilized in this paper were the results of experiments reported in the open literature¹⁻⁶. These included a total of 18 experiments and 75 individual radiation measurements. The pool diameters range from 1 to 50 m and fuels range from LNG to JP-5. All measurements were made with vertical targets at ground level. Data were not used here if the pool diameter was less than one meter, if less than three flux measurements were made in a particular test, or if large lip heights were employed. Table 1 summarizes the data utilized.

It is clear that other investigators have made radiant heat flux measurements but have not reported them in the open literature. In the

future it will be necessary to establish a mechanism to obtain unpublished results from investigators to expand the available database.

CORRELATIONS

For each experiment the best fit 'effective' emissive power was found. These results are shown in Table 1. Figure 1 shows a comparison of the incident radiant heat fluxes predicted using the 'effective' emissive powers in Table 1 with the measured heat fluxes. Since the 'effective' emissive powers were determined from the measured data, it is not surprising that the data are centered about the 45° angle line which indicates equality of the predicted and measured values. However, the small magnitude of the scatter about the line over two decades is a direct indication that the cylindrical flame shape is accurately portraying the decay in radiant heat flux with increasing distance from the pool fire.

Figure 2 shows a correlation of the data of Table 1 with the nondimensional distance from the

TABLE 1. Summary of Experiments

Investigator	Fuel	Diameter (m)	Data Points	'Effective' Emissive Power (kW/m ²)
Yamaguchi ¹	Kerosene	30.0	4	31
	Kerosene	50.0	4	16
Seeger ²	Fuel Oil	1.6	4	56
Yumota ³	Gasoline	1.0	5	41
	Gasoline	1.12	3	34
	Gasoline	1.5	3	44
	Gasoline	6.0	3	37
Dayan & Tien ⁴	JP-4	1.22	4	66
	JP-5	2.44	4	44
	JP-5	3.05	4	57
	JP-5	5.5	4	69
May & McQueen ⁵	LNG	14.6	4	61
	LNG	16.2	4	52
	LNG	18.3	4	54
	LNG	24.1	3	46
Hägglund & Persson ⁶	JP-4	1.13	6	85
	JP-4	2.25	5	90
	JP-4	11.28	7	60

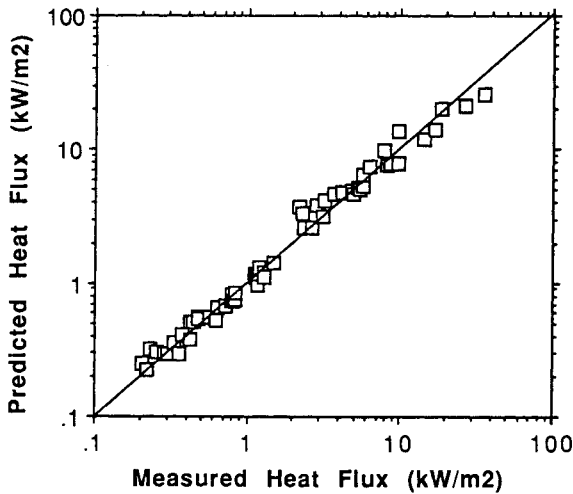


Figure 1. Comparison of calculated and measured incident radiant flux using the 'effective' emissive powers from Table 1. The solid line indicates equality of the predicted and measured heat fluxes.

pool center to the target location, L/D . Excluding the 50 m kerosene results, the data are well fit by the expression

$$\dot{q}'' = 15.4 \text{ kW/m}^2 \left(\frac{L}{D}\right)^{-1.59} \quad (8)$$

This expression is limited to vertical targets at ground level. While its generality is limited and it is not derived from any flame model, it may be useful for preliminary assessments.

Figure 3 shows the variation in the 'effective' emissive power with the 'effective' pool diameter.

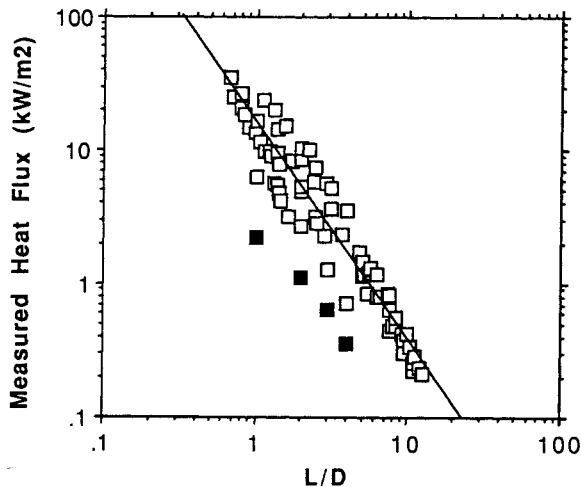


Figure 2. Measured incident radiant flux at ground level to a vertical target as a function of the distance from the pool center to the target normalized by the pool diameter. Solid symbols are 50 m diameter kerosene data. The solid line is Equation 8.

ter. The decay in the 'effective' emissive power results from the increase in the amount of black smoke enveloping the flame at larger pool diameters. Additional data points derived from Alger and Capner²⁷ are included in the figure. The data presented in Alger and Capner are in the form of faired curves and representative ranges for replicate tests. The range of results for each test configuration was very wide with variations in heat flux of a factor of two or more. These variations appear to be due to wind effects. The results from Alger and Capner used in Figure 3 represent average values. While Figure 3 shows significant scatter, there is a definite trend in the 'effective' emissive power with the 'effective' pool diameter. This variation can be represented as

$$E = 58 (10^{-0.00823 D}) [\text{kW/m}^2, \text{m}] \quad (9)$$

This expression is shown in Figure 3 as a solid line. This expression, which results from a least squares fit to the data, indicates that the 'effective' emissive power reduces from about 60 kW/m² at 1 m diameter to 20 kW/m² at about 60 m diameter.

The measurements of Hägglund and Persson⁶ of an emissive power of 20 kW/m² in the obscuring smoke clouds suggests that 'effective' emissive powers less than 20 kW/m² are not appropriate. While the 'effective' emissive powers for

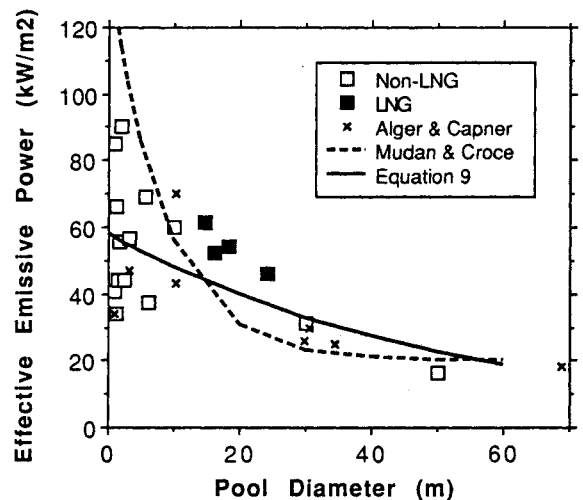


Figure 3. 'Effective' emissive power as a function of the pool diameter. Solid symbols are LNG experiments. The solid line is Equation 9, a curve fit to the present results, and the dashed line is Equation 10²³. The '+'s are results derived from Alger and Capner²⁷.

LNG included in Figure 3 are in good agreement with other fuels, the amount of obscuring smoke is known to be far less for LNG. Mizner and Eyre⁷ found 'effective' emissive powers of about 200 kW/m² for LNG pool fires. Since they did not publish their heat flux data, it is not possible to explore the reasons for the discrepancies between the present results and the Mizner and Eyre results. Until the discrepancies are resolved, it would be prudent to use the more conservative Mizner and Eyre values for LNG.

DISCUSSION

Over the years a number of investigators have suggested 'effective' emissive powers for use in predicting radiation from pool fires to external targets. These 'effective' emissive powers, summarized in Table 2, range from a low of 20 kW/m² to high of 220 kW/m².

Some of this divergence can be attributed to variations in the 'effective' emissive power with pool diameter due to the increasing prominence of black smoke clouds obscuring the luminous flaming zones of the fire.

Emissive powers of luminous flaming regions have been estimated by narrow angle radiometer measurements to be in the 120-200 kW/m²

range. Narrow angle radiometer measurements tend to be higher than the 'effective' emissive power because the narrow angle measurement does not see the whole flame. In general narrow angle measurements are made in the hottest, most luminous region of the flame. One might expect emissive powers measured by narrow angle instruments to overestimate the 'effective' emissive power. As such the narrow angle radiometer measurements of emissive power and 'effective' emissive powers cannot be used interchangeably.

Mudan and Croce²³ suggest the following expression for the 'effective' emissive power of gasoline, kerosene, and JP-4 flames.

$$E = E_{max} \exp(-sD) + E_s (1 - \exp(-sD)) \quad (10)$$

where $E_{max} = 140 \text{ kW/m}^2$, $E_s = 20 \text{ kW/m}^2$, and $s = 0.12 \text{ m}^{-1}$. The results of this investigation indicate that the variations with pool diameter are far less than indicated by this expression. In particular the 'effective' emissive power never approaches 140 kW/m², even at diameters as low as one meter.

It is significant that over half of the data used to establish Equation 10 is included in the current analysis. The differences in Equations 9 and 10 are the result of using different methods of estimating the flame geometry. This points out the importance of specifying a complete procedure for evaluating pool fire radiation. The data must be correlated and applied using the same procedures used to determine the 'effective' emissive power. Hence, reported 'effective' emissive powers are only useful if the methods used to determine them are fully reported.

While further detailed study of the variation of the 'effective' emissive power with diameter should be pursued, it is clear that previously recommended effective emissive powers are often far too high, some suggesting emissive powers 2 to 4 times the actual 'effective' emissive power. One may argue that choosing emissive powers conservatively is prudent in design. However, such safety factors should be introduced thoughtfully and explicitly.

Table 2. Summary of 'Effective' Emissive Powers from the Literature

Investigator	Emissive Power (kW/m ²)
Mizner & Eyre ⁷	
propane	43
LNG	203
Atallah <i>et al.</i> ²¹	97 - 118
DiNenno ²²	118 - 218
Mudan ¹⁹	42
Mudan & Croce ²³	
D=100 m	20
D=1 m	138
deRis ²⁴	118 - 218
Present Study	16 - 90

COMPARISON WITH THE MUDAN AND CROCE METHOD

In the *SFPE Handbook of Fire Protection Engineering*, Mudan and Croce²³ present a methodology for estimating the incident heat flux from a pool fire. In the case of no wind, their methodology uses the same assumed flame shape. They use a flame height correlation developed by Thomas from wood crib experiments, Equation 10 for the 'effective' emissive power, and explicitly use an atmospheric transmissivity correction. The present method and the Mudan & Croce methods are summarized in Table 2.

Figures 4 and 5 show comparisons of the present method and the Mudan & Croce method predictions, respectively, with the test results of References 1-4, and 6. Reference 5 is omitted because Mudan & Croce do not recommend their method for LNG. These figures clearly demonstrate that the present method better predicts the data than the Mudan & Croce method. This is to be expected since the present method is based on these data sets and the Mudan & Croce method is only partially based on these data sets. However, the Mudan & Croce method is overly conservative in most cases with some predicted fluxes 4-5 times the actual fluxes. Of the 60 data points in Figure 5, 20 were overpredicted by more than a factor of two. These data points are shown as solid symbols in Figure 5. The largest errors are made in the predictions for the 1 m diameter gasoline pool fire³. The largest errors for the present method are for the two near field data points for the 5.5 m JP-4 pool fires⁴, where the prediction is only about 60% of the actual value.

While the comparison of the two methods is clearly biased by the use of data from References 1-4 and 6, the present method clear-

ly performs better than the Mudan & Croce method. The large errors produced by the Mudan & Croce method can be reduced by the use of the present method.

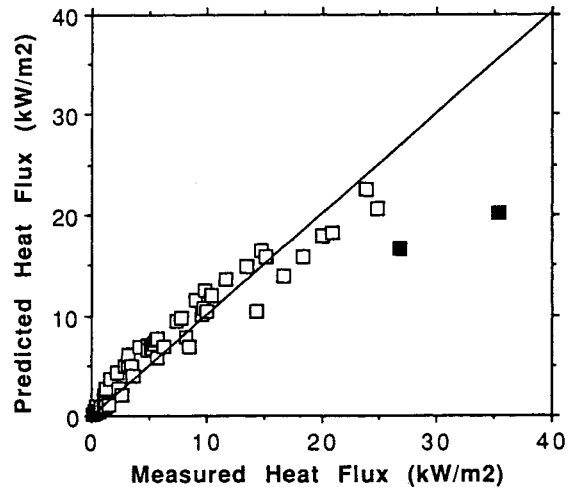


Figure 4. Comparison of the radiant heat flux predicted by the present method with the experimental data from References 1-4, 6. Solid symbols are data points which are underpredicted by more than 35%.

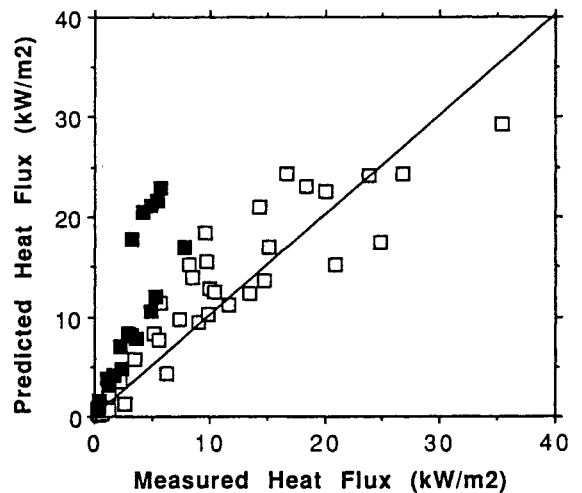


Figure 5. Comparison of the radiant heat flux predicted by the Mudan & Croce method with the experimental data from References 1-4, 6. Solid symbols are data points which are overpredicted by more than a factor of two.

Table 3. Comparison of Methods.

	Present Study	Mudan and Croce
Flame Shape	Upright Cylinder	Upright Cylinder
'Effective' Emissive Power	Equation 9	Equation 10
Flame Height Correlation (no wind)	Heskestad	Thomas
Atm. Absorption	Implicit	Explicit

RECOMENDED ALGORITHM

The following procedure is recommended for the evaluation of radiation from pool fires to external targets.

1. **Determine the heat release rate.** If direct experimental data are not available, Equation 4 and parameters given by Babrauskas¹⁸ are recommended for this determination. If parameters are not available in Babrauskas¹⁸ for the fuel in question, Equation 5 may be used.
2. **Flame Geometry.** The flame is taken to be a cylinder with the diameter of the pool. The height of the flame is given by Equation 3.
3. **Configuration Factor.** Use Equations 6 and 7.
4. **Effective Emissive Power.** Use Equation 9. In design situations it is appropriate to introduce a factor of safety into the 'effective' emissive power. A safety factor of two will give predicted heat fluxes in excess of any measurements used in this paper.
5. **Radiative Flux to Target.** Use Equation 1, $\dot{q}'' = E F_{12}$.

Note that this procedure does not include the effects of wind. Mudan¹⁹ recommends the use of a tilted cylinder flame shape for wind blown flames. See Reference 19 or 23 for methods of determining flame angle and the tilted cylinder configuration factor.

RADIATION TO THE POOL SURFACE

Orloff and deRis²⁵ have proposed a model for the prediction of radiation to the pool surface as a part of a methodology for the prediction of the pool burning rate. In order to facilitate calculations, it would be useful to streamline the existing model. The goal of this section is to develop a simple yet accurate alternative to the Orloff and deRis model.

The working equations for the Orloff and deRis model, Equations 11-13, form the starting point for the development.

$$\dot{q}_p'' = \sigma T^4 [1 - \exp(-kL_m)] \quad (11)$$

where

$$k = \frac{-\ln \left(1 - \frac{\chi_R \dot{Q}''' L_m}{3.6 \sigma T^4 \chi_A} \right)}{L_m} \quad (12)$$

$$\begin{aligned} \dot{Q}''' &= 1200 \text{ kW/m}^3 \\ \frac{L_m}{R} &= C_0 + C_1 \eta + C_2 \eta^2 + C_3 \eta^3 + C_4 \eta^4 + C_5 \eta^5 \quad (13) \\ \eta &= \frac{3V_f}{\pi R^3}, \quad V_f = \dot{Q}''' \end{aligned}$$

In these equations, $T=1200\text{K}$ is recommended by Orloff and deRis. It can be easily demonstrated that the results are completely independent of this choice. Combining Equations 11 and 12 yields

$$\dot{q}_p'' = \frac{\chi_R \dot{Q}''' L_m}{3.6 \chi_A} \quad (14)$$

The mean beam length, L_m , is given by

$$L_m = \frac{3.6 V_f}{A_b} \quad (15)$$

where V_f is the flame volume and A_b is the bounding surface area of the flame. Substituting Equation 15 into Equation 14 yields

$$\dot{q}_p'' = \frac{\chi_R \dot{Q}''' V_f}{\chi_A A_b} = \frac{\chi_R \dot{Q}_A}{\chi_A A_b} = \frac{\dot{Q}_R}{A_b} \quad (16)$$

Equation 16 simply says that the radiant flux to the pool surface is the total radiative output divided by the surface area of the flame.

The total radiation output of the flame can be easily determined. It remains to determine A_b . Equations 13 and 15 can be used for this purpose, but an explicit expression cannot be found for A_b by this approach.

Atreya²⁶ has developed an alternative curve fit to Orloff and deRis' data for L_m :

$$\frac{L_m}{R} = 0.425 \sqrt{\frac{3V_f}{\pi R^3}} \quad (17)$$

Equation 17 more simply and accurately repre-

sents Orloff and deRis' data than Equation 12. Combining Equations 15 and 17 yields

$$A_b = 8.67 \sqrt{V_f R} \quad (18)$$

Substituting Equation 18 and

$$\dot{Q}_R = (\chi_R/\chi_A) \dot{Q}_A = (\chi_R/\chi_A) \dot{Q}''' V_f$$

into Equation 16 gives

$$\dot{q}_p'' = \frac{\chi_R \sqrt{\dot{Q}'''}{8.67 \chi_A} \sqrt{\frac{\dot{Q}_A}{R}} \quad (19)$$

where $\dot{Q}''' = 1200 \text{ kW/m}^3$ and $\chi_R, \chi_A, \dot{Q}_A$ are properties of the pool fire. Equation 19 substitutes for the Orloff and deRis model (Equations 11-13). We see that the Orloff and deRis model is effectively $\dot{q}_p = \dot{Q}_R/A_b$ and an experimental correlation which gives A_b as a function of the flame volume and pool radius.

The Orloff and deRis model was developed from pool fire data with $D < 1 \text{ m}$. As such the use of Equation 19 should also be restricted to pools with diameters less than 1 m.

CONCLUSIONS

Through a review of available data for radiation from large pool fires to external targets, a procedure for predicting the incident radiant flux to a target outside the flame has been developed. This procedure is based on the classic cylindrical flame shape assumption and uses the flame height expression developed by Heskestad. There is a reduction in the 'effective' emissive power with increasing pool diameter. The method developed here is shown to yield more accurate results than the Mudan & Croce method²³.

The Orloff and deRis model for radiative heat transfer from the flame to the pool surface has been clarified and simplified.

REFERENCES

1. Yamaguchi, T., Wakasa, K., "Oil Pool Fire Experiment," *First International Symposium on Fire Safety Science*, Hemisphere Pub. Co., 1986, 911-918.
2. Seeger, P.G., "On the Combustion and Heat Transfer in Fires of Liquid Fuels in Tanks", *Heat Transfer in Fires*, Ed. Blackshear, P.L., Section 2, Chapter 3, Scripta Book Co., Washington, D.C., 1974, 95-126.
3. Yumota, T., "Fire Spread Between Two Oil Tanks", *J. of Fire Flam.*, **8**, 1977, 494.
4. Dayan, A., Tien, C.L., "Radiant Heating from a Cylindrical Fire Column", *Comb. Sci. Tech.*, **9**, 1974, 41-47.
5. May, W., McQueen, W. G., "Radiation from Large Liquefied Natural Gas Fires", *Comb. Sci. Tech.*, **7**, 1973, 51-56.
6. Hägglund, B., Persson, L., "The Heat Radiation from Petroleum Fires", FOA Report C 20126-D6(A3), Stockholm, Sweden, 1976.
7. Mizner, G.A., Eyre, J.A., "Radiation from Liquefied Gas Fires on Water", *Comb. Sci. Tech.*, **35**, 1983, 33-57.
8. Moorhouse, J., "Scaling Criteria for Pool Fires Derived from Large Scale Experiments", *I.Chem. E. Symposium Series No. 71*, pp. 165-179.
9. Mudan., K., Croce, P.A., "A Thermal Radiation Model for LNG Trench Fires", ASME Paper 84-WA/HT-75, 1984.
10. Raj, P.K., "Analysis of JP-4 Fire Test Data and Development of a Simple Fire Model", ASME Paper 81-HT-17, 1981.
11. Burgess, D., Hertzberg, M., "Radiation from Pool Flames", in *Heat Transfer in Flames*, Ed. Afgan, N.H. and Beer, J.M., Scripta Book Co., Washington D.C., 1974, 413-430.
12. Wayne, F.D., Kinsella, K., "Spectral Emission Characteristics of Large Hydrocarbon Pool Fires", AMSE Paper 84-WA/HT-74, 1984.
13. Schönbacher, A., Brötz, W., Balluff, C., Göck, D., Schieb, N., "Erforschung von Schadenfeuern Flüssiger Kohlenwasserstoffe als Beitrag zur Sicherheit von Chemieanlagen", *Chem. Ing. Tech.*, **57**, 1985, 823-834.
14. Schönbacher, A., Brötz, W., Balluff, C., Riedel, G., Kettler, A., Schieb, N., "Visualization of Organized Structures in Buoyant Diffusion Flames", *Ber. Bunsenges Phys. Chem.*, **89**, 1985, 595-603.

NOMENCLATURE

- | | |
|--|---|
| <p>15. Heskestad, G., "Luminous Height of Turbulent Diffusion Flames", <i>Fire Safety Journal</i>, 5, 1983, 103-108.</p> <p>16. Beyler, C.L., "Fire Plumes and Ceiling Jets", <i>Fire Safety Journal</i>, 11, 1986, 53-75.</p> <p>17. Babrauskas, V., "Estimating Large Pool Fire Burning Rates", <i>Fire Technology</i>, 19, 1983, 251-261.</p> <p>18. Babrauskas, V., "Burning Rates", <i>SFPE Handbook of Fire Protection Engineering</i>, Ed. P. DiNunno <i>et al.</i>, National Fire Protection Association, Quincy MA, 1988, Section 2, Chapter 1., 1-15.</p> <p>19. Mudan, K.S., "Thermal Radiation Hazards from Hydrocarbon Pool Fires", <i>Prog. Energy Comb. Sci.</i>, 10, 1984, 59-80.</p> <p>20. Steward, F.R., "Black Body View Factors", Appendix 1, <i>Heat Transfer in Fires</i>, Ed. Blackshear, P.L., Section 4, Scripta Book Co., Washington, D.C., (1974), 409-431.</p> <p>21. Atallah, S., Allan, S., "Safe Separation Distances from Liquid Fuel Fires", <i>Fire Technology</i>, 7, 1971, 47-56.</p> <p>22. DiNunno, P., "Simplified Radiation Heat Transfer Calculations for Large Open Hydrocarbon Fires", SFPE Technical Report 82-9, 1982.</p> <p>23. Mudan, K., Croce, P., "Fire Hazard Calculations for Large Open Hydrocarbon Fires", <i>SFPE Handbook of Fire Protection Engineering</i>, Ed. P. DiNunno <i>et al.</i>, National Fire Protection Association, Quincy MA, 1988, Section 2, Chapter 4, 45-87.</p> <p>24. deRis, J., "Fire Radiation, a Review", <i>Seventh Symposium (International) on Combustion</i>, Combustion Institute, (1978), 1003.</p> <p>25. Orloff, L., deRis, J., "Froude Modeling of Pool Fires", <i>Nineteenth Symposium (International) on Combustion</i>, Combustion Institute, 1982, 885-895.</p> <p>26. Atreya, A., <i>Pyrolysis, Ignition, and Fire Spread on Horizontal Surfaces of Wood</i>, Ph.D. Thesis, Harvard University, 1983.</p> <p>27. Alger, R.S., Capner, E.L., <i>Basic Relationships in Military Fires, Phases III, V, VI, and VII</i>, DOD-AGFSRL-75-4, NSWC and Stanford Research Institute, May 1975.</p> | <p>A - pool surface area, [m²]</p> <p>D - pool diameter, [m]</p> <p>E - 'effective' flame emissive power, [kW/m²]</p> <p>F_{12} - configuration factor between the flame and target, [-]</p> <p>H - flame height, [m]</p> <p>k - flame extinction coefficient, [1/m]</p> <p>L - distance from the pool centerline, [m]</p> <p>L_m - mean beam length of the flame, [m]</p> <p>\dot{m}'' - mass volatilization rate per unit area of pool, [kg/m²s]</p> <p>\dot{m}''_{∞} - \dot{m}'' in the limit of large D, [kg/m²s]</p> <p>\dot{q}'' - incident radiative flux to the target, [kW/m²]</p> <p>\dot{q}''_p - incident radiative flux to the pool surface, [kW/m²]</p> <p>\dot{Q}_A - actual heat release rate, [kW]</p> <p>\dot{Q}_R - radiative output of the pool fire, [kW]</p> <p>\dot{Q} - heat release rate of pool fire, [kW]</p> <p>\dot{Q}''' - actual heat release rate per unit volume of flame, 1200 kW/m³</p> <p>R - pool radius, [m]</p> <p>T - effective radiation temperature of the pool fire, [K]</p> <p>V_f - flame volume, [m³]</p> <p>χ_R - radiative fraction, [-]</p> <p>χ_A - combustion efficiency, [-]</p> <p>Δh_c - lower heat of combustion of the fuel, [kJ/kg]</p> <p>Δh_v - heat required to heat the fuel to the boiling temperature and volatilizing the fuel, [kJ/kg]</p> |
|--|---|